Hyperonic matter in neutron star

P. K. Sahu[a*] and A. Ohnishi[a]

[a] Division of Physics, Hokkaido university, Sapporo 060-0810, Japan

We discuss appearance and role of hyperons in neutron star matter with recent compiled nuclear equation of state from heavy-ion collisions. We also discuss different hyperon couplings from analysis of various experimental data on hypernuclei. We find that the sigma baryons do not appear in the neutron star matter, when it experiences a strong repulsive potential. However, the change in maximum mass of the neutron stars is insignificant against the different hyperon couplings.

1. INTRODUCTION

In spite of more than two decades of work, the nuclear equation of state (EOS), which is required in calculation of neutron star properties is uncertain due to various reasons. The EOS at high baryon densities is one source of uncertainties, because it sensitively depends on short range nucleon-nucleon interaction. Furthermore, weak decay of neutrons into hyperons may be energetically allowed at high densities and the neutron matter may contains hyperons at such large baryon densities. If hyperons are likely to exist in high density matter, then it must be noted that the interaction of hyperons with other baryons is not well understood and the EOS is therefore uncertain.

In this discussion, we use an extended version of the relativistic mean field model with momentum dependent forces, which are taken phenomenologically in the relativistic transport model in heavy-ion collisions [1]. The EOS was then derived by using momentum dependent constraints in the nuclear potentials [2]. We employ the same EOS in the neutron star calculation, where the composition of the star matter consists of lambdas, sigmas, cascades, neutrons, protons, electrons and muons.

2. NEUTRON STAR MATTER

The EOS of neutron star matter is calculated in the frame work of the mean-field theory using covariant Lagrangian [3,4] given below.

$$\begin{aligned}\mathcal{L} &= \sum_i \bar{\psi}_i(i\gamma^\mu\partial_\mu - m_i + g_{\sigma i}\sigma + g_{\omega i}\omega_\mu\gamma^\mu - g_{\rho i}\rho^a_\mu\gamma^\mu T_a)\psi_i \\ &\quad -\frac{1}{4}\omega^{\mu\nu}\omega_{\mu\nu} + \frac{1}{2}m^2_\omega\omega_\mu\omega^\mu + \frac{1}{2}(\partial_\mu\sigma\partial^\mu\sigma - m^2_\sigma\sigma^2) - \frac{1}{4}\rho^a_{\mu\nu}\rho^{\mu\nu}_a + \frac{1}{2}m^2_\rho\rho^a_\mu\rho^\mu_a \\ &\quad -\frac{1}{3}bm_N(g_{\sigma N}\sigma)^3 - \frac{1}{4}c(g_{\sigma N}\sigma)^4 + \sum_l \bar{\psi}_l(i\gamma^\mu\partial_\mu - m_l)\psi_l. \qquad (1)\end{aligned}$$

*PKS was supported by the Japan Society for the Promotion of Science (ID No. P98357), Japan.

The Lagrangian includes n, p, Λ, Σ^+, Σ^-, Σ^0, Ξ^- and Ξ^0 (denoted by subscript i), electrons and muons (denoted by subscript l) and σ, ω and ρ mesons (given by σ, ω^μ and $\rho^{a\mu}$, respectively). The Lagrangian includes third and fourth order self-interactions of the σ field. The meson fields interact with baryons through linear coupling and these are different for nonstrange and strange baryons. The parameters $g_{\sigma N}$, $g_{\omega N}$, $g_{\rho N}$, b and c are determined by fitting saturation density, binding energy, effective nucleon mass, compression modulus and symmetry energy coefficient at nuclear matter density (cf. the NL3 parameter set from Table I in Ref. [5,2]).

The EOS is obtained by adopting mean field ansatz, where the mesons develop nonzero vacuum expectation values ($\bar{\sigma}$, $\bar{\omega}$ and $\bar{\rho}^3$, respectively) in presence of baryons. Assuming that the baryon densities are uniform, e.g., the time components of $\bar{\omega}$ and $\bar{\rho}^a$ with $\bar{\sigma}$ are nonzero. Then the effective masses and chemical potentials for baryons are defined as $\bar{m}_i = m_i - g_{\sigma i}\bar{\sigma}$ and $\bar{\mu}_i = \mu_i - g_{\omega i}\bar{\omega} - I_{3i}g_{\rho i}\bar{\rho}^3$, respectively, where I_{3i} is the value of the z-component of the isospin of the baryon i.

Throughout calculation, we incorporate momentum-dependent form factors at the vector and scalar vertices in a form given as [2], $\bar{\omega}(p) = \bar{\omega}\frac{p^2-\Lambda_{v1}^2}{p^2+\Lambda_{v2}^2}$ and $\bar{\sigma}(p) = \bar{\sigma}\frac{p^2-\Lambda_{s1}^2}{p^2+\Lambda_{s2}^2}$, respectively, where the cutoff parameters are Λ_{v1}=0.37 GeV, Λ_{v2}=0.9 GeV, Λ_{s1} =0.71 GeV and Λ_{s2} =1.0 GeV. The values of cutoff parameters are chosen to describe properly the Schrödinger-equivalent potential and flow data up to AGS energies [1]. We note that the form factor in the vector vertices make a nonlinear dependence of the vector potential on the baryon density, and as a result, the vector interaction is weak at high baryon density. It has been observed that the strength of the repulsive potential should be reduced considerably at high density to describe the flow data [1]. A detailed discussion is given in Ref. [2].

In neutron star matter, the concentrations of each particle can be determined by using the condition of chemical equilibrium under weak interactions and charge neutrality (assuming that neutrinos are not degenerate):

$$\begin{aligned}
&\mu_p = \mu_{\Sigma^+} = \mu_n - \mu_e, \quad \mu_\Lambda = \mu_{\Sigma^0} = \mu_{\Xi^0} = \mu_n, \quad \mu_{\Sigma^-} = \mu_{\Xi^-} = \mu_n + \mu_e, \mu_\mu = \mu_e; \\
&n_p + n_{\Sigma^+} = n_e + n_\mu + n_{\Sigma^-} + n_{\Xi^-}.
\end{aligned} \tag{2}$$

The total baryon density is defined as $n_B = \sum_i n_i$, where n_i stands for number density of the i th particle.

Taking all these factors into account in our calculation, then neutron star matter EOS, such as the energy density ε and pressure P can be calculated from the diagonal components of the stress-energy tensor, which are given as follows:

$$\begin{aligned}
\varepsilon &= \frac{1}{2}m_\omega^2\bar{\omega}_0^2 + \frac{1}{2}m_\rho^2(\bar{\rho}_0^3)^2 + \frac{1}{2}m_\sigma^2\bar{\sigma}^2 + \frac{1}{3}bm_N(g_{\sigma N}\bar{\sigma})^3 + \frac{1}{4}c(g_{\sigma N}\bar{\sigma})^4 \\
&\quad + \sum_i E_{FG}(\bar{m}_i, \bar{\mu}_i) + \sum_l E_{FG}(m_l, \mu_l), \\
P &= \frac{1}{2}m_\omega^2\bar{\omega}_0^2 + \frac{1}{2}m_\rho^2(\bar{\rho}_0^3)^2 - \frac{1}{2}m_\sigma^2\bar{\sigma}^2 - \frac{1}{3}bm_N(g_{\sigma N}\bar{\sigma})^3 - \frac{1}{4}c(g_{\sigma N}\bar{\sigma})^4 \\
&\quad + \sum_i P_{FG}(\bar{m}_i, \bar{\mu}_i) + \sum_l P_{FG}(m_l, \mu_l).
\end{aligned} \tag{3}$$

In above equations, the P_{FG} and E_{FG} are the relativistic non-interacting pressure and energy density of the fermions.

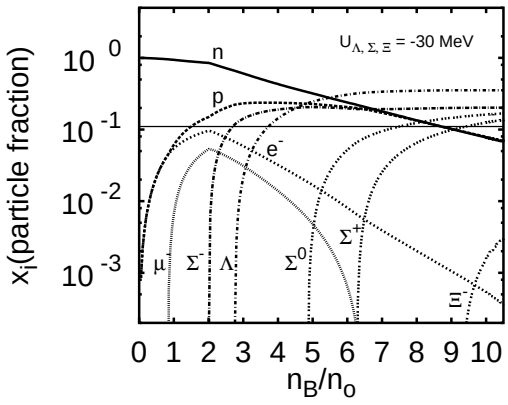

Figure 1. Particle fraction as a function of baryon density in units of saturation density.

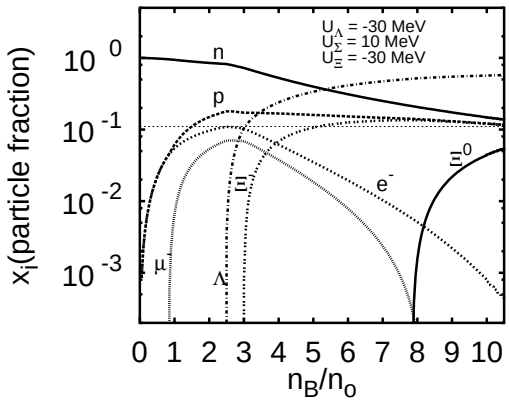

Figure 2. Same as in figure 1. In this case the Σ disappear due to strong repulsion.

3. RESULTS

The hyperon couplings (ratio of meson-hyperon and meson-nucleon) are not well known. These cannot be determined from nuclear matter properties since the nuclear matter does not contain hyperons. Furthermore, analysis of experimental data on hypernuclei does not fix these parameters in a unique way. Thus in nuclear matter, we adjust the ratio of the hyperon-meson and nucleon-meson couplings for σ, ω and ρ mesons, respectively, by assuming (i) the potentials experienced by all hyperons same as that of Λ, -30 MeV, (ii) Σ experiences $+10$ MeV (strong repulsive) [6] and all other hyperons are -30 MeV and (iii) Σ, Ξ and Λ hyperons experience $+10$ MeV, -16 MeV (less attractive) [7,8] and -30 MeV, respectively. Here in all three cases, values of the hyperon couplings are between 0.65 and 0.95.

We illustrate three hyperon coupling cases in Figures 1$-$3. In all these figures, particle fractions ($x_i = n_i/n_B$) are displayed against baryon density in units of n_0. In Fig. 2, the Σ is absent because of the strong repulsion [6]. Similarly, the Ξ starts appearing at high density due to less attraction [7,8] in Fig. 3. The other hyperon fractions are adjusted accordingly when Σ is absent (case (ii)) and Ξ experience less attraction (case iii)) to maintain charge neutrality in neutron star matter. These can be observed by comparing Figs. 1$-$3. The similar type of figures have been shown in Ref. [9] by using an effective interaction model. It is worthwhile to mention here that small amount of Σ can appear again in neutron star matter, when the nuclear symmetry energy is chosen to be very small.

The maximum neutron star masses as a function of central densities are shown in Fig. 4. The solid curve (*npl*) is neutron star matter without hyperons and (i), (ii) and (iii) curves are with hyperons as discussed in Figs. 1$-$3, respectively. It is seen that hyperons significantly reduce maximum neutron star mass from $2.35M_\odot$ to $2.0M_\odot$. However, against different hyperon couplings as discussed in Figs. 1$-$3, the change in

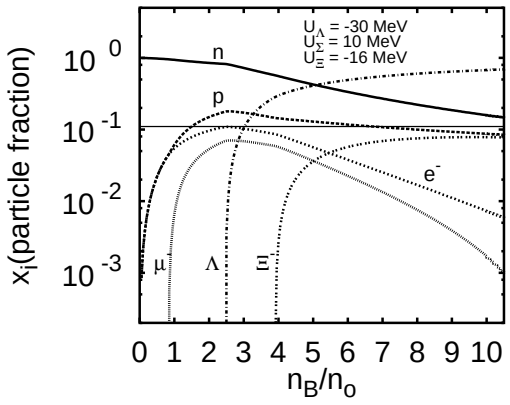

Figure 3. Same as in figure 2. The Ξ^- appears at high density due to less attraction.

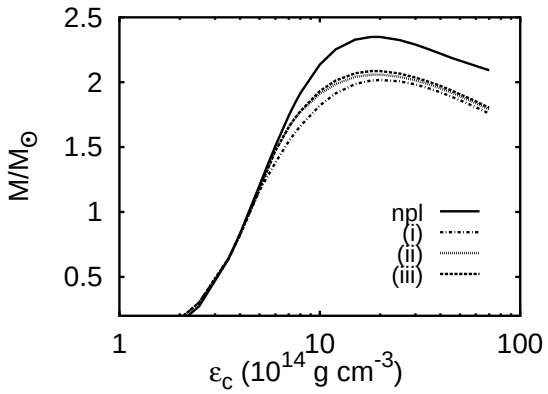

Figure 4. Gravitation mass as a function of central energy density.

maximum mass limit is insignificant, which is clear from Fig. 4. In all cases, the maximum neutron star masses are in recent observational limit [10]. Recently, it has been pointed out that, the presence of hyperons in the neutron star with different hyperon couplings (hyperon-hyperon potentials) interestingly play significant role in the super-fluidity of hyperon-mixed neutron star and hyperon- pairing gaps [11].

In conclusion, we used recent compiled nuclear EOS from heavy-ion reactions to describe the neutron star properties with hyperons. In the strange baryon sector, we considered different hyperon couplings from the analysis of various experimental data and found that the sigma baryons are absent in the neutron star matter, when these experience strong repulsive force. In our conclusion, we noticed that these different uncertainties of hyperon couplings do not change the maximum mass of the neutron star significantly.

REFERENCES

1. P.K. Sahu et al., Nucl. Phys. A672 (2000) 376.
2. P.K. Sahu, Phys. Rev. C62 (2000) 045801.
3. N.K. Glendenning, Astrophys. J. 293 (1985) 470.
4. S.K. Ghosh et al., Z. Phys. A352 (1995) 457.
5. A. Lang et al., Z. Phys. A340 (1991) 207.
6. J. Dabrowski, Phys. Rev. C 60 (1999) 025025.
7. T. Fukuda et al., Phys. Rev. C 58 (1998), 1306.
8. P. Khaustov et al., Phys. Rev. C 61 (2000), 054603.
9. S. Balberg and A. Gal, Nucl. Phys. A625 (1997), 435.
10. H. Heiselberg, Proc. of the 10th Int. Conf. on Recent Progress in Many-Body Theories, World Scientific, (1999); nucl-th/9912002.
11. T. Takatsuka, S. Nishizaki, Y. Yamamoto and R. Tamagaki, Prog. Theor. Phys. 105 (2001), 179.